Journal of Geochemical Exploration 175 (2017) 138–147

Contents lists available at ScienceDirect

Journal of Geochemical Exploration

journal homepage: www.elsevier.com/locate/gexplo

Factorial kriging analysis and pollution evaluation of potentially toxic elements in soils in a phosphorus-rich area, South Central China

Chenchang Du [a], Enfeng Liu [b], Nengcheng Chen [a,c], Wei Wang [a,c,*], Zhifan Gui [d], Xian He [e]

[a] State Key Laboratory of Information Engineering in Surveying, Mapping and Remote Sensing, Wuhan University, Wuhan 430079, China
[b] State Key Laboratory of Lake Science and Environment, Nanjing Institute of Geography and Limnology, Chinese Academy of Sciences, Nanjing 210008, China
[c] Collaborative Innovation Center of Geospatial Technology, Wuhan 430079, China
[d] College of Urban and Environment Sciences, Hubei Normal University, Huangshi 435002, China
[e] Dalian Academy of Reconnaissance and Mapping Co. Ltd, Dalian 116061, China

ARTICLE INFO

Article history:
Received 7 August 2016
Revised 2 January 2017
Accepted 18 January 2017
Available online 19 January 2017

Keywords:
Potentially toxic elements
Pollution
Source
Spatial variation
Factorial kriging analysis

ABSTRACT

Identifying spatial variations of potentially toxic elements at different spatial scales and their contamination conditions is important for soil management and remediation. Utilizing a 1 km × 1 km sampling grid, a total of 615 soil samples were collected from a phosphorus-rich area of South Central China and determined for arsenic (As), cadmium (Cd), cobalt (Co), chromium (Cr), copper (Cu), nickel (Ni), lead (Pb), vanadium (V), and zinc (Zn) concentrations. Factorial kriging analysis (FKA), enrichment factor (EF), and potential ecological risk (RI) were used to examine scale-dependent correlations between the elements, identify factors of multi-scale spatial variations, and assess pollution status, respectively. The results indicate that only the mean concentrations of As, Cd, and Pb exceeded the background levels. Based on EF method, the pollution levels of As, Cd, and Pb were assessed as middle or high, and according to the RI values, 11.2% of the study area was under considerable potential ecological risk. Through linear model of co-regionalization (LMC) fitting, spatial multi-scale variations of elements could be modeled as the sum of a nugget effect, an exponential structure (3 km), and a spherical structure (15 km). At the short-range scale, spatial variations of Co, Cr, Cu, Ni, and V were controlled by parent materials, whereas that of As, Pb, Cd, and Zn were related to human influence, such as phosphorus-related industrial activities and river pollution. At the long-range scale, parent materials were the dominant factors regulating the spatial variations of all elements.

© 2017 Elsevier B.V. All rights reserved.

1. Introduction

Soil is not only necessary for vegetation growth and acts as a sink for contaminants, but also interacts with the atmosphere, hydrosphere, and biosphere (Cai et al., 2015; Mihailović et al., 2015). Because of rapid urbanization and industrialization, soil pollution has become a pressing problem. Among numerous kinds of soil pollutants, potentially toxic elements are particularly concerning because of their non-biodegradability and persistence (Islam et al., 2015; Mihailović et al., 2015). Excessive accumulation of potentially toxic elements in soils not only has adverse effects on the soil ecosystem but may also harm human health as it passes through the food chain (Schneider et al., 2016).

Concentrations of potentially toxic elements in soils are mainly influenced by parent materials and human activities (Sollitto et al., 2010). It has been found that the functional ranges of parent materials and human activities on spatial variations of elements differ (Benamghar and Gómez-Hernández, 2014; Zhao et al., 2015). For example, industrial wastewater affecting element variability generally has a short-range scale of influence, whereas parent materials are likely to operate over longer distances (Benamghar and Gómez-Hernández, 2014; Lv et al., 2013). Thus, potentially toxic elements should be studied in a scale dependent way. Factorial kriging analysis (FKA), a multivariate geostatistical method, is particularly promising for interpreting spatial multi-scale variations of elements. It employs co-regionalization analysis to partition the spatial variations of elements into numerous spatial components corresponding to different spatial scales (Goovaerts, 1992; Schneider et al., 2016). Combined with principal component analysis (PCA), this method can be used to examine the spatial correlations between potentially toxic elements and identify the sources of spatial variations of elements at each spatial scale (Chilès and Delfiner, 1999; Lin et al., 2010).

With rapid economic development during recent decades, soil element pollution has become an important problem in China (Chen et al., 2011). Numerous surveys related to soil elements have been

* Corresponding author at: State Key Laboratory of Information Engineering in Surveying, Mapping and Remote Sensing, Wuhan University, Wuhan 430079, China.
E-mail address: pingfandesj@163.com (W. Wang).

http://dx.doi.org/10.1016/j.gexplo.2017.01.010
0375-6742/© 2017 Elsevier B.V. All rights reserved.

performed (Liu and Ma, 2012; Wu and Zhang, 2010), but few studies have considered the element variability across multiple scales, especially in areas with phosphate-rich rock. In this study, the phosphorus-rich area of Zhongxiang City, South Central China, was selected. The phosphorus chemical industry in the study area has made significant contributions to regional economic and social development (Chen et al., 2012). However, due to a lack of pollution control during phosphoric acid production, and the absence of standardized construction methods for phosphogypsum slag sites, environmental problems, especially soil element contamination, are becoming increasingly severe. The primary aims of this study were to: 1) investigate concentrations of potentially toxic elements in soils and assess their pollution levels and potential ecological risk; and 2) identify the dominant factors regulating spatial variations of elements at different scales. The results can be used to establish policies for protecting the soil quality in other areas with phosphate-rich rock.

2. Materials and methods

2.1. Study area

The study area is located in the northwest of Zhongxiang City, in the central region of Hubei Province, China (Fig. 1). It includes three towns: Huji, Linkuang and Shuanghe. This area lies within 31°11′–31°33′ N and 112°7′–112°31′ E, and covers about 777 km^2. It belongs to the northern subtropical zone, and is characterized by a monsoonal climate with four distinct seasons. The average annual temperature and rainfall are 15.9 °C and 970 mm, respectively. The elevation varies from 37 to 403 m above sea level; mountainous area is located in the northwest and north (Fig. 2a). Parent materials in the study area contain phosphorite in the northwestern mountainous area, pyroclastic rock in the northern mountainous area, pluvial and alluvial deposition in the northern plain area, and glutenite in the western and northern parts of the

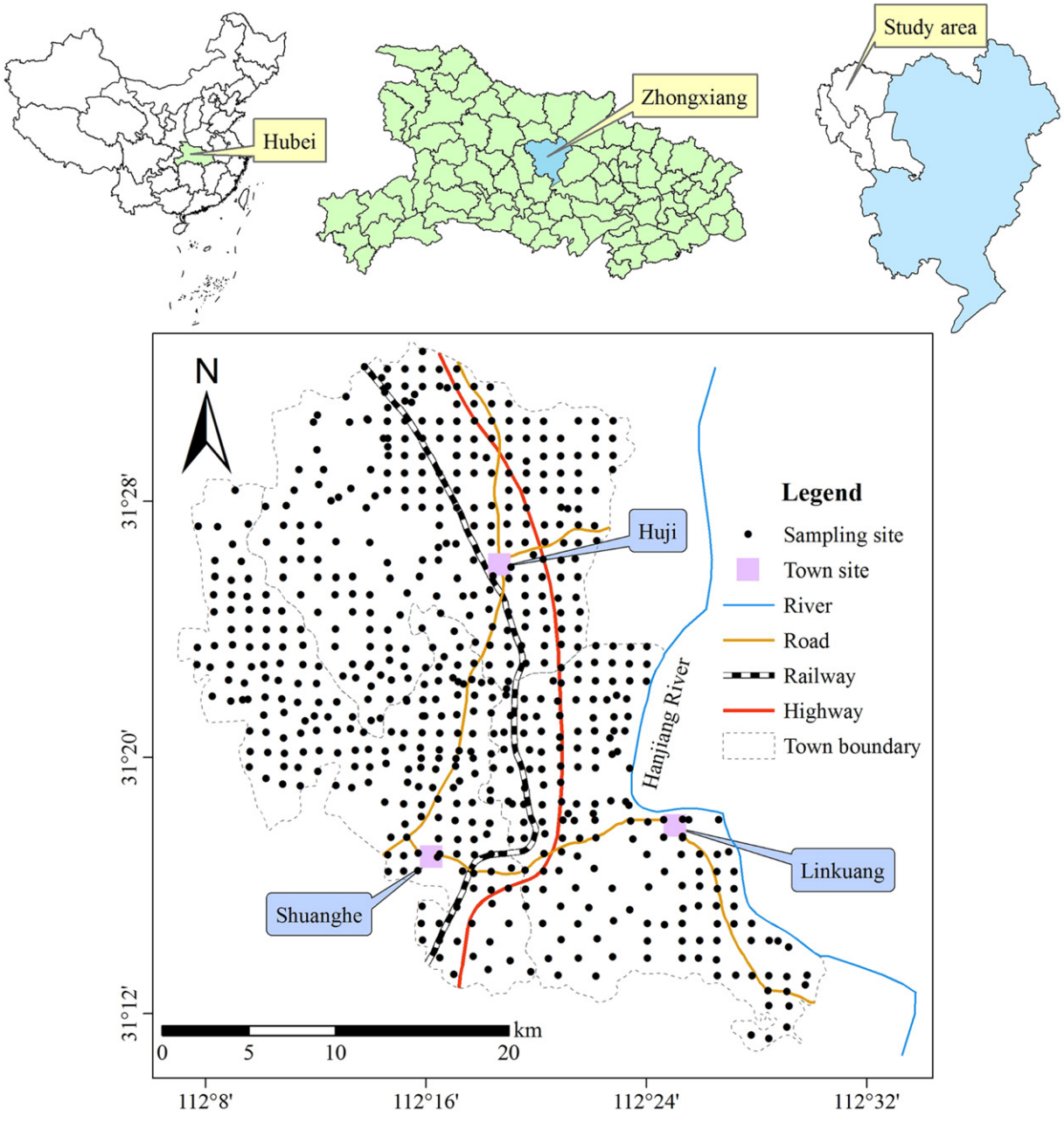

Fig. 1. The location of study area and distribution of sampling sites.

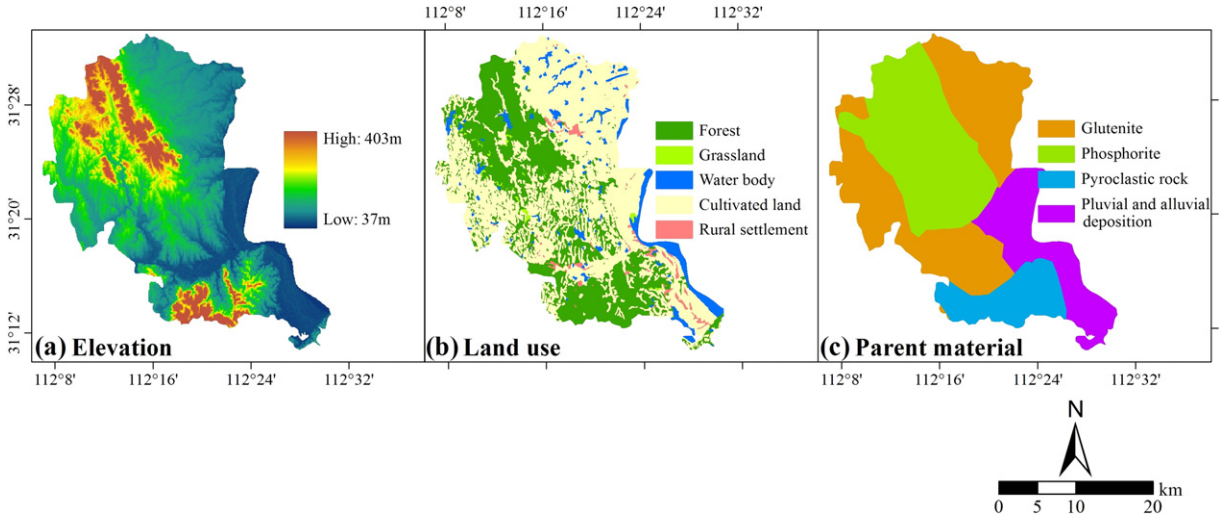

Fig. 2. Topography, land use types, and parent materials of the study area.

study area (Fig. 2c). Forest and grassland cover about 41.5% and 0.9% of the total area, respectively, mainly in the mountainous area, and cultivated land accounts for 50.1% of the total area (Fig. 2b). The Hanjiang River flows alongside the southeastern part of the study area, and is a major water resource for agricultural, domestic, and industrial uses in this area.

The study area is rich in phosphate-bearing rock, and there is a long history of mining these resources. As an important area for phosphate fertilizer production, this region now has numerous phosphate chemical enterprises and is well known in China for its phosphorus products (e.g., monoammonium phosphate, diammonium phosphate, ammonium bicarbonate, and ammonium nitrate). The biggest industrial park of the study area, the Jingxiang Phosphorus Industrial Park, lies 2 km west of the seat of the Huji town government.

2.2. Soil sampling and chemical analysis

A total of 615 soil samples (0–20 cm depth) were collected in the study area in 2014. The sample sites were based on a 1 km × 1 km grid, with each grid square containing one or two sampling sites (Fig. 1). Each sample was a mixture of five sub-samples, randomly collected from around each sampling point with a stainless steel spade. The sampling coordinates were recorded with a Global Positioning System (GPS) device. The samples were air-dried at room temperature. After removing stones and other debris, portions of the soil samples (about 100 g each) were ground with an agate grinder to pass a 100 mesh, and stored in plastic bags prior to analysis.

A small portion of each sample was digested using HNO_3–HCl–$HClO_4$ and the concentrations of cadmium (Cd), cobalt (Co), chromium (Cr), copper (Cu), nickel (Ni), lead (Pb), vanadium (V), and zinc (Zn) were determined using inductively coupled plasma–atomic emission spectrometry (ICP-AES). Another small portion of each sample was digested in aqua regia and the concentrations of arsenic (As) were measured using atomic fluorescence spectrometry (AFS). The accuracy and precision of the analysis were controlled using blanks, replicates, and a standard reference soil sample, GSS-1 (Geochemical Standard Soil). The analytical precision of replicate samples was within ± 10%, and the errors between the measured and certified values of the elements were below 5%.

2.3. Assessment of pollution levels and ecological risk

There are many different indices used for assessing the pollution status of potentially toxic elements, such as the pollution index (PI), the integrated pollution index (IPI), the geoaccumulation index (I_{geo}), the enrichment factor (EF), and the potential ecological risk index (RI) (Mirzaei et al., 2014). Because using the EF reduces the influence of grain size effect on element concentrations and improves quantification of the extent of enrichment, the EF was used in this study to understand the pollution levels of the different elements. It is computed with the following equation (Liu and Shen, 2014; Wu et al., 2015):

$$EF = (C_a/C_r)_{sample}/(C_a/C_r)_{background} \quad (1)$$

where EF is the enrichment factor of element a, C_a is the concentration of element a, and C_r is the concentration of a reference element. For calculating the EF values, V was chosen as the reference element because V usually originates from the parent materials of the soil, and the V concentrations of soils in the study area are similar to the regional background level (Wu et al., 2015). The background concentrations of potentially toxic elements in soils of Hubei Province were selected as the background levels (Liu and Ma, 2012). Based on conventional classification standards and the characteristics of the EF (Wu et al., 2015; Yuan et al., 2012), pollution levels of elements are classified as deficient to minimal (EF < 1.5), middle (1.5 ≤ EF < 3), or high (EF ≥ 3).

First developed by Hakanson (1980), the potential ecological risk index (RI) is evaluated based on the toxic-response factors of elements and has been utilized by numerous researchers to assess the potential ecological risk posed by potentially toxic elements (Islam et al., 2015; Wang et al., 2014). The value of the RI is computed as follows:

$$RI = \sum_{i=1}^{n} E_r^i = \sum_{i=1}^{n} T_r^i \times C_f^i = \sum_{i=1}^{n} T_r^i \times C_0^i/C_n^i \quad (2)$$

where RI is sum of the ecological risk indices of elements in soils, E_r^i is the single ecological risk index, T_r^i is the toxic-response factor, C_f^i is the pollution coefficient of an element, and C_0^i and C_n^i are the concentrations of element i in the evaluated samples and reference background. The toxic-response factors for As, Cd, Co, Cr, Cu, Ni, Pb, and Zn are 10, 30, 5, 2, 5, 5, 5, and 1, respectively (Yuan et al., 2014). The value of E_r^i is classified as low risk (E_r^i<40), moderate risk (40≤E_r^i<80), considerable risk (80≤E_r^i<160), high risk (160≤E_r^i<320), or very high risk (E_r^i≥320) (Hakanson, 1980). The following thresholds are suggested for RI values: RI < 65, low ecological risk; 65 ≤ RI < 130, moderate ecological risk; 130 ≤ RI < 260, considerable ecological risk; and RI ≥ 260, high ecological risk (Hakanson, 1980; Luo et al., 2007).

Table 1
Descriptive statistics for soil element concentrations (mg kg^{-1}).

Element	As	Cd	Co	Cr	Cu	Ni	Pb	V	Zn
Mean	15.17	0.20	17.00	85.75	30.39	38.31	33.10	107.65	76.46
Maximum	48.70	0.58	32.90	119.00	64.70	70.40	53.80	164.70	142.30
Minimum	5.50	0.06	7.90	50.60	16.00	19.10	17.80	61.60	43.00
SD	5.08	0.10	3.48	11.97	5.67	7.43	9.30	16.73	16.74
CV (%)	33.48	48.52	20.51	14.03	18.68	19.37	30.89	15.45	21.91
Skewness	2.52	1.40	0.26	−0.18	1.30	−0.01	0.92	0.60	0.94
Kurtosis	10.71	1.92	1.42	0.27	4.93	0.77	3.71	1.18	1.16
Background[a]	10.50	0.11	14.60	79.00	28.20	34.70	25.70	104.20	77.50
Guideline[b]	25.00	0.30	–	300.00	100.00	50.00	300.00	–	250.00
Samples exceeding guideline value (%)	4.48	14.02	–	0.00	0.00	4.92	0.00	–	0.00

[a] Background: background value of potentially toxic element in soils of Hubei Province (Liu and Ma, 2012).
[b] Guideline: Environmental Quality Standard for Soils in China (Grade II), i.e., the maximum allowable concentration of elements in farmland soils, including arable land (vegetable, tea, and fruit) and grazing land, formulated by the State environmental protection administration of China (SEPAC, 1995).

2.4. Factorial kriging analysis

Factorial kriging analysis was employed to analyze the multi-scale structures of potentially toxic elements. This method facilitates linear model co-regionalization (LMC) fitting to identify important information related to interrelationships between elements at different scales (Lin et al., 2016; Lv et al., 2015). In LMC, the auto- and cross-variograms of a set of n variables are modeled as sums of variograms $\gamma_{ij}^{u}(h)$ at each scale u, and can be described linearly by basic models $g^{u}(h)$. The LMC can be shown in matrix from as:

$$\gamma(h) = \left[\gamma_{ij}(h)\right] = \sum_{u=1}^{Ns} B^{u} g^{u}(h) \tag{3}$$

where $\gamma(h)$ states the $n \times n$ variogram matrix (diagonal and other elements representing auto- and cross-variograms, respectively), Ns is the total number of the spatial structures, and B^{u} is the co-regionalization matrix, which describes the relationships between different variables for the uth scale. This procedure was carried out using weighted least-squares under the constraint that the co-regionalization matrices for all structures were positive semi-definite.

Following the experience with modeling the variograms of the n variables, a nested spatial structure, including a nugget effect, an exponential structure, and a spherical structure, was constructed and can be expressed as:

$$\gamma_{ij}(h) = b_{ij}^{0} \text{ for } h = 0 \tag{4}$$

$$\gamma_{ij}(h) = b_{ij}^{0} + b_{ij}^{1}\left(1 - e^{-h/a_1}\right) + b_{ij}^{2}\left[\frac{3}{2}\left(\frac{h}{a_2}\right) - \frac{1}{2}\left(\frac{h}{a_2}\right)^{3}\right] \tag{5}$$

for $0 < h \le a_2$ km

$$\gamma_{ij}(h) = b_{ij}^{0} + b_{ij}^{1} + b_{ij}^{2} \text{ for } h > a_2 \text{ km} \tag{6}$$

where b_{ij}^{0} represents the nugget variances, b_{ij}^{1} states the sill for short-range structure, b_{ij}^{2} is the sill for long-range structure, a_1 and a_2 state the distance parameters of the short- and long-range structures.

Based on the co-regionalization matrices, the structural correlation coefficient r_{ij}^{u} between different elements can be defined as:

$$r_{ij}^{u} = b_{ij}^{u} / \sqrt{b_{ii}^{u} \times b_{jj}^{u}} \tag{7}$$

where b_{ij}^{u} is the value at position (i, j) in the matrix B^{u} at the particular spatial scale u.

Principal component analysis was separately performed on each B^{u} matrix to generate a set of principal components (Nanos et al., 2015). The correlation circles were then employed to describe the correlation coefficients between the first two principal components (PCs) and the original variables at each scale. The FKA was carried out using the gstat R package (Pebesma, 2004).

Each original variable can be broken down into the sum of various spatial components corresponding to different spatial scales; the mapping of spatial components was carried out with ArcGIS 10.0 software using ordinary cokriging.

When data distributions are highly skewed, the presence of outliers may make LMC fitting complicated. Usually, logarithm transformation is employed to reduce the skewness coefficients of data (Liu et al., 2013), although Box–Cox transformation generally performs better than logarithm transformation (Zhang et al., 2009). Therefore, in this study, Box–Cox transformation was adopted and after transformation, variables were standardized with means of zero and unit variance.

3. Results and discussion

3.1. Descriptive statistics

A descriptive summary of element concentrations in the soil samples is given in Table 1. The average concentrations of the elements

Table 2
Results of ANOVA for element concentrations by parent materials and land use types (mg kg^{-1}).

		Ns	As	Cd	Co	Cr	Cu	Ni	Pb	V	Zn
Land use type	Rural settlement	16	15.34b	0.33a	17.26a	86.44a	33.59a	39.47a	32.31b	115.99a	89.39a
	Cultivated land	373	14.17b	0.20b	16.45b	84.70b	29.48b	37.02b	31.78b	106.95a	74.70c
	Nature vegetation	226	16.66a	0.19b	17.88a	87.44a	32.74a	40.36a	34.24a	108.22a	78.46b
	F		19.94[b]	15.89[b]	12.34[b]	3.75[a]	5.18[b]	15.07[b]	8.02[b]	2.45	8.68[b]
Parent material	Alluvial deposition	106	14.00c	0.28a	17.74a	90.32a	33.55a	40.81a	30.58c	123.37a	89.85a
	Pyroclastic rock	43	15.42b	0.19b	17.80a	90.19a	31.23b	40.92a	33.03a	108.84b	79.92b
	Glutenite	266	13.56c	0.17b	15.99b	81.54c	28.56c	35.44b	31.09b	101.13c	69.26c
	Phosphorite	200	17.88a	0.19b	17.77a	87.96b	30.95b	40.24a	34.30a	107.74b	78.21b
	F		34.64[b]	46.57[b]	14.01[b]	22.49[b]	23.50[b]	26.40[b]	34.46[b]	57.01[b]	50.05[b]

Values marked by the same letter are not significant.
[a] Significant at the 0.05 level.
[b] Significant at the 0.01 level.

decreased in the following order: V > Cr > Zn > Ni > Pb > Cu > Co > As > Cd. The average concentrations of Co, Cr, Cu, Ni, V, and Zn were close to the background levels in soils of Hubei Province, which indicates only slight human inputs for these elements (Liu and Ma, 2012). The mean concentrations of As, Cd, and Pb were 1.44, 1.82, and 1.28 times as high as the background levels, which suggests that these elements may be influenced by human inputs (Liu and Ma, 2012). The coefficient of variation (CV) for element concentrations showed a wide range, from 14.03% to 48.52%. Cadmium had the highest CV value, reaching 48.52%, which indicates that Cd may have the highest probability of being affected by anthropogenic inputs (Chen et al., 2008). Chromium had the lowest CV value at 14.03%, which implies that Cr was fairly homogeneously distributed across the study area (Cai et al., 2015). Some elements, such as As and Cd, had skewness values significantly higher than zero. Therefore, in FKA, for the purpose of eliminating the skewness values of elements and facilitating LMC fitting, Box–Cox transformation was carried out on the original data set.

According to the Environmental Quality Standard for Soils in China (SEPAC, 1995), the mean concentrations of As, Cd, Cu, Ni, Pb, and Zn all fell under the guideline values. For As and Cd, about 4.5% and 14.0% of the samples, respectively, exceeded their corresponding guideline values. In addition, 4.92% of the samples exceeded the guideline value for Ni, but this might be attributed to a high background Ni value (Table 1). In general, there was slight element contamination in the study area.

3.2. Comparison of element concentrations between land use types and parent materials

To examine the total variation associated with environmental factors, analysis of variance (ANOVA) was employed to compare element concentrations between different groups (i.e., land uses and parent materials). ANOVA results by land use types and parent materials are presented in Table 2. There were significant differences for all element concentrations except for V between various land use types. The mean concentrations of Cd and Zn in rural settlement were significantly higher than those associated with other land uses, which may be attributed to intensive human activities. The mean concentrations of As, Pb, Zn, Co, Cr, Cu, and Ni in cultivated land were significantly lower than in natural vegetation, including grassland and forest, which may be associated with the high geological background concentrations and indicates that agricultural practices had insignificant influence on concentrations of these elements.

The mean concentrations of As and Pb in soils from phosphorite and pyroclastic rock were significantly higher than those associated with other parent materials, which indicates influence of these parent materials. The mean concentrations of Co, Cr, Cu, Ni, and V in soils from glutenite were significantly lower than those from the other parent materials, indicating that parent materials affected these element concentrations. For Cd and Zn, the mean concentrations in soils from pluvial and alluvial deposition were higher.

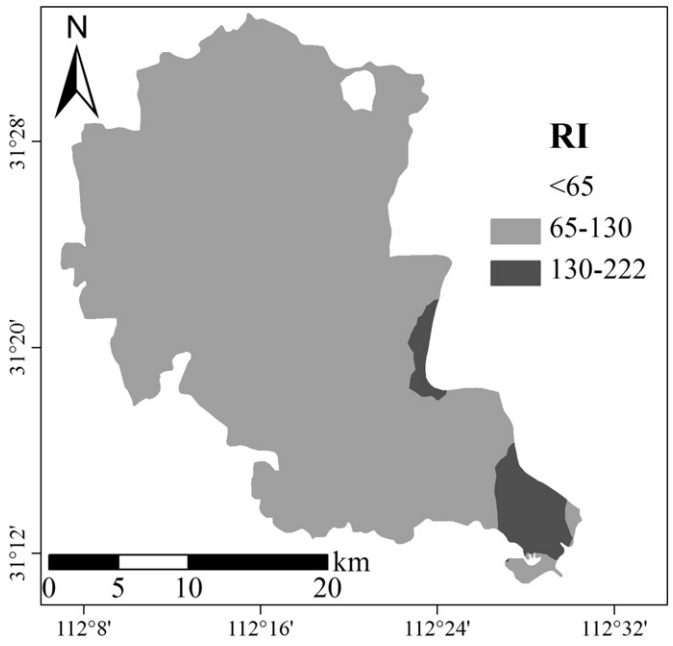

Fig. 3. Potential ecological risk (RI) map for elements.

3.3. Pollution and ecological risk assessment

The EF values for elements are shown in Table 3. The mean EF values for Co, Cr, Cu, Ni, and Zn were 1.1, 1.1, 1.1, 1.1, and 1.0, respectively. About 96.7%, 99.8%, 99.0%, 99.3%, and 98.9% of the samples, respectively, were at the deficient to minimal pollution level for Co, Cr, Cu, Ni, and Zn, indicating that there were no apparent pollution problems associated with these elements. The EF values for Pb were between 0.6 and 2.2, with an average value of 1.3, and 12.2% of the samples were at a middle pollution level, which suggests that there may be Pb pollution in some soils. Respectively, the mean EFs for As and Cd were 1.4 and 1.7, and

Table 3
Statistical results for the enrichment factor (EF) and the potential ecological risk (RI) of elements.

Element	EF			Percentage of samples with each pollution level (%)		
	Min	Max	Mean	Low	Middle	High
As	0.6	5.1	1.4	74.3	23.7	2.0
Cd	0.4	6.2	1.7	48.6	46.3	5.1
Co	0.5	2.1	1.1	96.7	3.3	0.0
Cr	0.8	1.9	1.1	99.8	0.2	0.0
Cu	0.6	2.3	1.1	99.0	1.0	0.0
Ni	0.6	2.2	1.1	99.3	0.7	0.0
Pb	0.6	2.2	1.3	87.8	12.2	0.0
Zn	0.6	2.4	1.0	98.9	1.1	0.0

Potential ecological risk for elements

Element	Potential ecological index range (E_r^i)	Mean (E_r^i)	SD
As	5.2–46.4	14.4	4.8
Cd	15.5–151.8	52.2	25.4
Co	2.7–11.3	5.8	1.2
Cr	1.3–3.0	2.2	0.3
Cu	2.8–11.5	5.4	1.0
Ni	2.8–10.1	5.5	1.1
Pb	3.5–10.5	6.6	1.8
Zn	0.6–1.8	1.0	0.2
RI	49.3–221.5	92.2	27.2

Table 4
Parameters for LMC and the ratios of nugget or sill to total variation for each scale.

	Parameters of LMC			Ratio of nugget or sill to total variation for each scale		
	Nugget effect	Sill of short-range	Sill of long-range	Non-spatial scale	Short-range scale	Long-range scale
As	0.345	0.591	0.180	0.309	0.530	0.161
Cd	0.367	0.397	0.255	0.360	0.390	0.250
Co	0.655	0.203	0.307	0.562	0.174	0.264
Cr	0.599	0.249	0.173	0.587	0.244	0.169
Cu	0.583	0.352	0.091	0.568	0.343	0.089
Ni	0.590	0.164	0.326	0.546	0.152	0.302
Pb	0.344	0.705	0.088	0.303	0.620	0.077
V	0.562	0.109	0.359	0.546	0.106	0.349
Zn	0.391	0.317	0.337	0.374	0.303	0.322

Table 5
Structure correlation coefficients between elements.

	Element	As	Cd	Co	Cr	Cu	Ni	Pb	V	Zn
General correlation	As	1.00								
	Cd	−0.11	1.00							
	Co	0.58	−0.06	1.00						
	Cr	0.53	−0.11	0.67	1.00					
	Cu	0.42	0.26	0.51	0.68	1.00				
	Ni	0.57	0.00	0.76	0.89	0.71	1.00			
	Pb	0.63	−0.04	0.50	0.34	0.36	0.32	1.00		
	V	0.42	0.07	0.65	0.86	0.69	0.82	0.20	1.00	
	Zn	0.32	0.44	0.42	0.46	0.76	0.59	0.20	0.59	1.00
Nugget effect	As	1.00								
	Cd	−0.05	1.00							
	Co	0.27	0.05	1.00						
	Cr	0.49	0.10	0.59	1.00					
	Cu	0.13	0.35	0.42	0.62	1.00				
	Ni	0.40	0.15	0.70	0.88	0.62	1.00			
	Pb	0.31	0.00	0.45	0.37	0.29	0.234	1.00		
	V	0.37	0.24	0.60	0.90	0.66	0.80	0.31	1.00	
	Zn	−0.05	0.54	0.39	0.68	0.67	0.68	0.06	0.77	1.00
Short scale (3 km)	As	1.00								
	Cd	0.16	1.00							
	Co	0.32	−0.58	1.00						
	Cr	0.23	−0.61	0.58	1.00					
	Cu	0.51	0.06	0.44	0.45	1.00				
	Ni	0.52	−0.51	0.48	0.82	0.60	1.00			
	Pb	0.67	0.13	0.53	0.55	0.56	0.57	1.00		
	V	0.41	−0.39	0.14	0.79	0.48	0.74	0.41	1.00	
	Zn	0.78	0.66	0.01	−0.26	0.53	0.04	0.56	−0.09	1.00
Long scale (15 km)	As	1.00								
	Cd	−0.24	1.00							
	Co	0.58	0.56	1.00						
	Cr	0.49	0.64	0.88	1.00					
	Cu	−0.01	0.94	0.72	0.85	1.00				
	Ni	0.52	0.57	0.97	0.93	0.77	1.00			
	Pb	0.67	−0.75	0.10	−0.12	−0.58	0.06	1.00		
	V	0.02	0.90	0.765	0.83	0.97	0.78	−0.53	1.00	
	Zn	0.03	0.85	0.73	0.84	0.96	0.82	−0.49	0.92	1.00

about 25.7% and 51.4% of the samples were at the middle or high pollution level for these elements, which indicates the presence of As and Cd pollution in these soils.

The results for potential ecological risk are shown in Table 3, and the risk map is depicted in Fig. 3. The E_r^i values for the nine elements decreased in the following order: Cd > As > Pb > Co > Ni > Cu > Cr > Zn. The E_r^i values for Co, Cr, Cu, Ni, Pb, and Zn were lower than 40 in all samples, which indicates that these elements posed a low ecological risk. In contrast, the E_r^i values for As and Cd showed broader ranges, 5.2–46.4 and 15.5–151.8, respectively. For As, 0.7% of the samples indicated a moderate ecological risk, and for Cd, 62.9% of the samples showed a moderate or considerable ecological risk. The RI values were used to represent the ecological risk posed by various elements. RI values were below 130 for 88.8% of the study area, which indicates that the majority of the study area had a low or moderate ecological risk. The remaining 11.2% of the study area was characterized by RI values between 130 and 260, which indicates that the potentially toxic elements in this area may pose a considerable ecological risk. The highest RI values were found in the area adjacent to the Hanjiang River (Fig. 3). It was apparent that Cd was the key element representing the potential ecological risk of element contamination in the study area (Table 3 and Fig. 3).

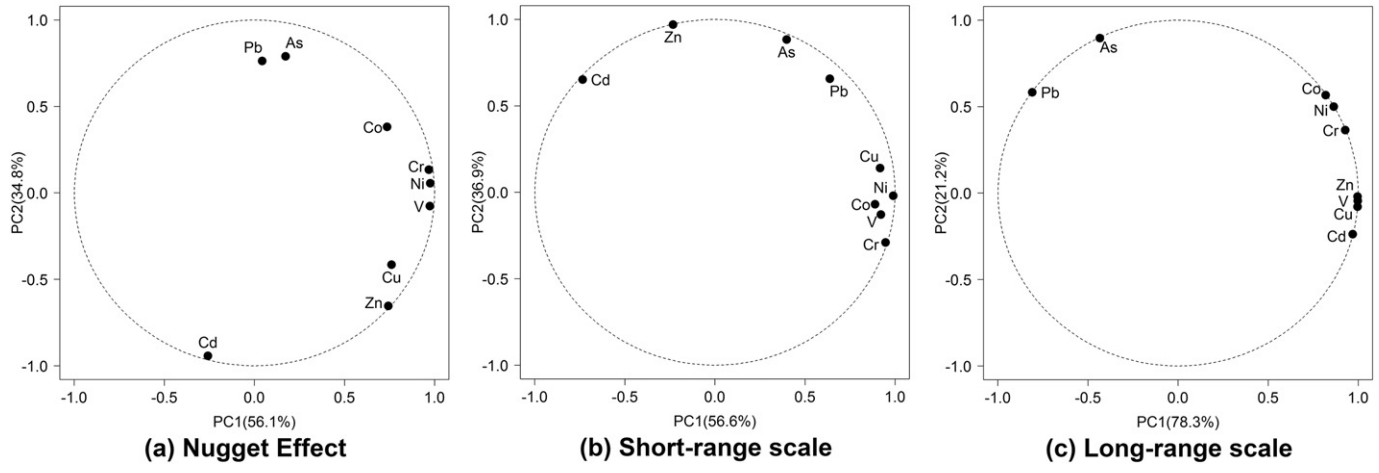

Fig. 4. Correlation circles for elements at each spatial scale.

3.4. Structure variation analysis

3.4.1. LMC fitting

FKA was carried out to analyze multi-scale spatial characteristics of the nine potentially toxic elements at 615 sampling points. Based on variogram analysis, 3 km and 15 km were selected as the distance parameters (a_1 and a_2 in Eqs. (4)–(6)) of short- and long-range structures. Then, the procedure of LMC fitting was carried out.

The parameters for LMC and the ratio of nugget or sill to total variation for all spatial structures are presented in Table 4. All elements had a large component of the nugget effect, ranging from 30.3% to 58.7%. Some previous studies have employed nugget/sill ratios to assess the spatial dependence of potentially toxic element concentrations with two thresholds (0.25 and 0.75) and ascribed high spatial dependence on intrinsic factors (e.g., parent materials, soil types, and topography) and low spatial dependence on extrinsic factors (e.g., human contamination) (Cambardella et al., 1994; Wang and Lu, 2011). In the present study, it was found that Co, Cr, Ni and V, which had low CV values and were assessed at the deficient to minimal pollution level based on the EF method had the highest nugget/sill ratios, and that As and Pb, which had high CV values and were apparently polluted, had the lowest nugget/sill ratios, which is inconsistent with these studies (Li et al., 2013; Wang and Lu, 2011). This discrepancy may exist because nugget variances are commonly caused by measurement error and especially spatial variations that cannot be detected within the shortest sampling resolution because of coarse sampling intervals (Lv et al., 2014; Xu et al., 2014). Therefore, the nugget/sill ratio should be used with caution to associate observations with intrinsic or extrinsic factors based on spatial dependence. Short-range structure was the largest component for As, Cd and Pb; it accounted for 53.0%, 39.0%, and 62.0% of the total variance of each of these elements, respectively, which indicates the apparent influence of human activities on short-range spatial

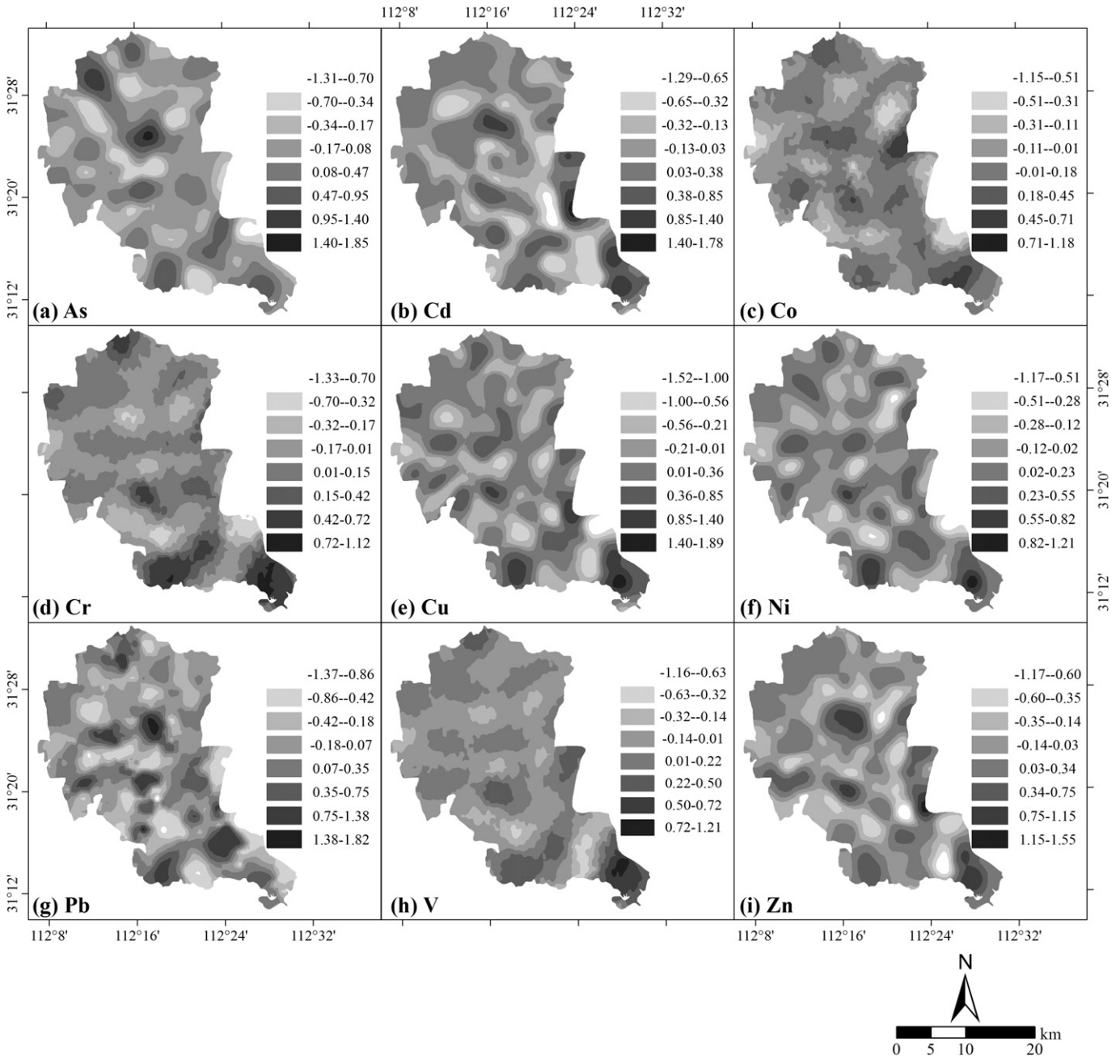

Fig. 5. Cokriged maps of spatial components at the short-range scale.

variations. As Table 4 shows, long-range structure was the smallest component for all nine elements.

3.4.2. Multi-scale interrelationships between elements

Structure correlation coefficients between elements at different scales are shown in Table 5. Traditional correlation coefficients do not reflect the real interrelationships between variables because they average out distinct changes in correlation structures at different spatial scales and encompass measurement errors inherent in the nugget effect (Liu et al., 2013). For example, the Spearman's nonparametric correlation coefficient between Cd and V was 0.07, whereas after the nugget effect was filtered out, the correlation coefficients at the short- and long-range scales were −0.39 and 0.90, respectively.

The correlations between elements at the long-range scale were highest, which is because the nugget effect and short-range variances were filtered out. At the nugget effect, short- and long-range scales, As and Pb showed significant positive correlations with each other, which indicates that these two elements may share common sources. Cobalt, Cr, Cu, Ni, and V were also highly correlated at all spatial scales, indicating that the concentrations of these elements were influenced by the same factors. Cadmium and Zn showed strong correlations with Co, Cr, Cu, Ni, and V at the long-range scale, whereas weaker correlations with these elements for the nugget effect and short-range scale may be because Cd and Zn concentrations were locally impacted by human inputs. It can be concluded that the correlation coefficients between elements in the study area depended on the spatial scale.

3.4.3. Principal component analysis at different spatial scales

Principal component analysis was carried out on the co-regionalization matrices to summarize the relationships among elements at

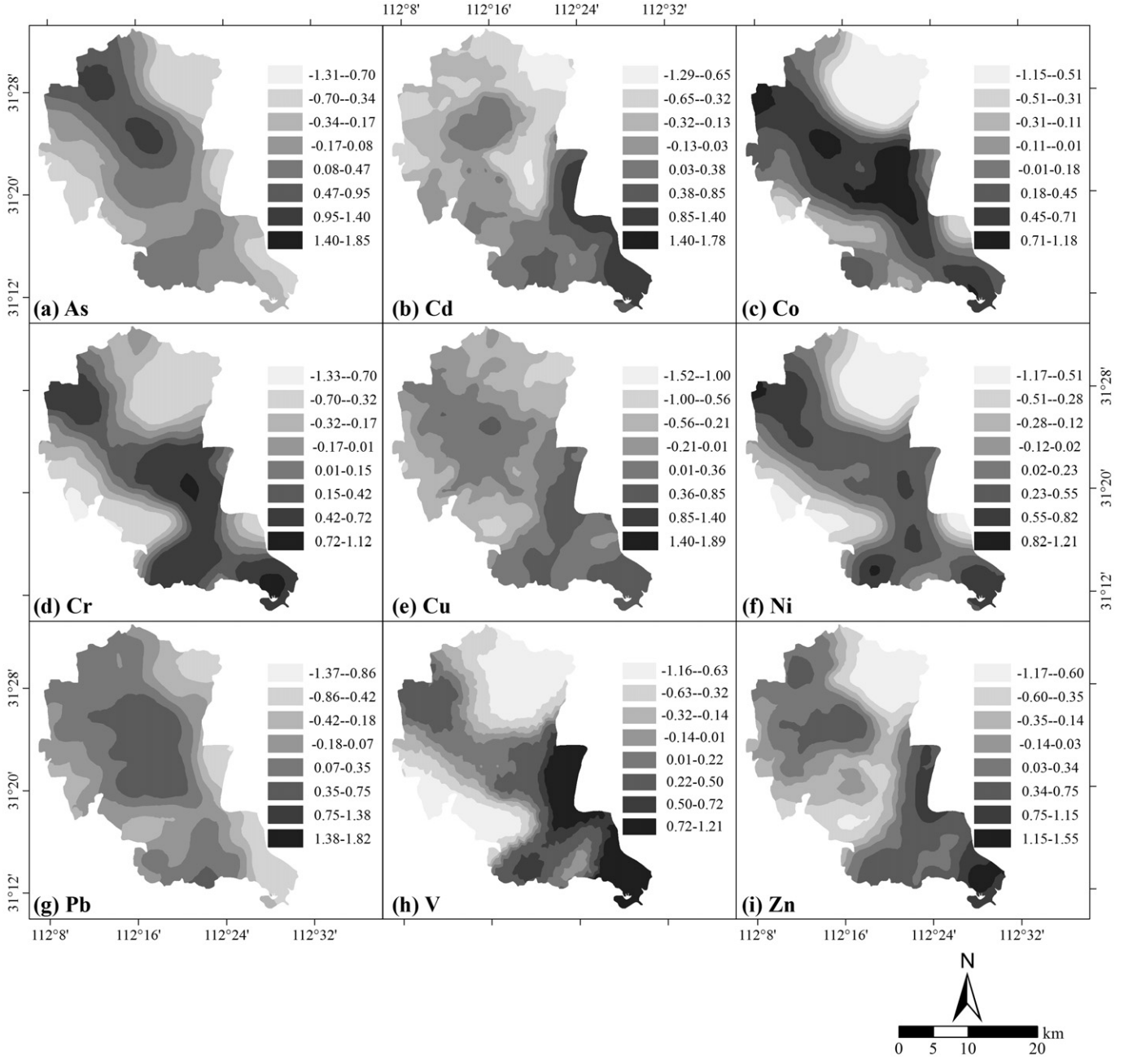

Fig. 6. Cokriged maps of spatial components at the long-range scale.

different spatial scales, and the correlations between the first two PCs and the elements at each spatial scale are displayed in the unit circle (Fig. 4). As discussed above, nugget variances contain the variances within the sampling intervals and measurement errors, both of which cannot be eliminated in structure analysis. Therefore, at the nugget effect scale the element sources cannot be accurately identified based on the results of principal component analysis.

At the short-range scale, PC1 explained 56.6% of the total variance, significantly positive loadings in Co, Cr, Cu, Ni and V and highly negative loadings in Cd and Zn. PC2 accounted for 36.9% of the total variance, with highly positive loadings of As, Cu, Pb, and Zn. At the long-range scale, PC1 accounted for 78.3% of the total variance, and had highly positive loadings with Cd, Co, Cr, Cu, Ni, V, and Zn, whereas PC2 explained 21.2% of the total variance, and has higher loadings for As and Pb.

At the short-range scale, Co, Cr, Cu, Ni, and V were sorted into the same group, which can be considered to be attributed to natural sources. The concentrations of Co, Cr, and Ni in soils are controlled by their concentrations in parent rock, which has been clearly illustrated by many studies (Facchinelli et al., 2001; Nanos and Rodríguez Martín, 2012). Moreover, their human inputs are generally lower than the background concentrations in the soils (Facchinelli et al., 2001). The spatial component maps show that the hotspots of Co, Cr, Cu, Ni, and V at the short-range scale were not located at mining sites or residential areas, but seemed to be random, which may be related to small patches of parent rock (Fig. 5c, d, e, f, and h) (Lv et al., 2014). In addition, the mean concentrations of Co, Cr, Cu, Ni, and V were approximately equivalent to their background levels, and their CV values were low, which indicates there were no apparent human inputs for these elements. Therefore, it can be concluded that Co, Cr, Cu, Ni, and V at the short-range scale were mainly influenced by natural factors.

At the short-range scale, As, Pb, Cd, and Zn were associated with anthropogenic sources. As discussed above, 25.7%, 51.4%, and 12.2% of the samples had As, Cd, and Pb, respectively, at the middle or high pollution level based on the EF assessment, and As, Cd, and Pb also had higher CV values. These features clearly demonstrate the influence of anthropogenic sources. Short-range variations of As, Pb, Cd, and Zn had a common hotspot with higher values in the northern part of the study area (Fig. 5a, b, g, and i), which was consistent with the location of the Jingxiang Phosphorus Industrial Park. Therefore, it can be inferred that this hotspot of As, Pb, Cd, and Zn was linked to phosphorus-related industrial activities. During phosphoric acid production, wastewater and residues that contain many potentially toxic elements (including these four elements) are released into the soil. In addition, large amounts of phosphogypsum are sometimes stacked in the vicinity of phosphate rock mining enterprises, which also affect short-range variations of As, Pb, Cd, and Zn through runoff and soil erosion. Another hotspot of short-range variations of As was located in the vicinity of old arsenic enterprises in the northwestern part of the study area (Fig. 5a). Although these arsenic enterprises were closed, complete elimination of As pollution in this area will require a significant amount of time. The surrounding regions of the Hanjiang River had higher values of short-range variations of Cd and Zn, which indicates the influence of this River on these elements (Fig. 5b and i). The water quality of the Hanjiang River is markedly affected by wastewater discharge from cities along the river such as Xiangyang City, approximately 80 km upriver from the study area, which contributes 53% of the wastewater discharged into the river (Lei et al., 2015). It has been reported that the sediments of the middle and lower Hanjiang River are severely polluted with Cd and Zn (Gao et al., 2011). Unavoidably, irrigation with water from the Hanjiang River may cause Cd and Zn pollution in the soil. Therefore, the high values of short-range variations of Cd and Zn in the soils adjacent to the Hanjiang River were mainly attributed to the long-standing practices of irrigation using water from the Hanjiang River.

Many previous studies have found that agricultural practices have significant influence on short-range variations of Cd, Pb, and Zn in agricultural area due to the application of pesticides and fertilizer (Lv et al., 2015; Rodríguez et al., 2008). However, in this study, at the short-range scale, the spatial components of Cd, Pb, and Zn levels in cultivated land did not show significantly higher values (Figs. 2b and 5b, g, and i), which is confirmed by with the results of ANOVA for land use types (Table 2). In addition, the distributions of short-range variations of Cd, Pb, and Zn in cultivated land were similar to those of Cr and Ni, which generally are not affected by agricultural practices (Nanos and Rodríguez Martín, 2012). Therefore, it can be concluded that agricultural practices did not show significant influence on short-range variations of Cd, Pb, and Zn.

At the long-range scale, Cd, Co, Cr, Cu, Ni, V, and Zn were classified into the same group and were controlled by parent materials. Through spatial overlay analysis, it was found that the higher values of spatial variations of Cd, Co, Cr, Cu, Ni, V, and Zn were mainly in soils originated from phosphorite, pluvial and alluvial deposition, and pyroclastic rock, whereas low values were associated with glutenite parent rock, which indicates the lithologic nature of Cd, Co, Cr, Cu, Ni, V, and Zn at the long-range scale (Figs. 2c and 6b, c, d, e, f, h, and i). This inference is confirmed by the results of ANOVA for parent materials (Table 2). At the long-range scale, As and Pb showed little correlation with Cd, Co, Cr, Cu, Ni, V, and Zn and also were natural in origin. The higher values of long-range variations for As and Pb were mainly in soils from phosphorite and pyroclastic rock (Figs. 2c and 6a and g), which indicates the influence of natural factors on these two elements, and is also confirmed by the results of ANOVA for parent materials (Table 2). Generally, parent materials with wide distributions operate at longer distances to dominate long-range variability when short-range variations influenced by human sources are filtered out (Lv et al., 2014; Nanos and Rodríguez Martín, 2012). Previous studies have also indicated that long-range variations of elements coincide with bedrock distribution and are mainly influenced by parent materials (Davies, 1997; Lv et al., 2013).

4. Conclusions

The spatial multi-scale variations of potentially toxic elements in a phosphorus-rich area, Zhongxiang, South Central China were revealed based on the analysis of 615 topsoil samples. The average concentrations of Co, Cr, Cu, Ni, V, and Zn were similar to the regional levels in local soils, whereas the mean concentrations of As, Cd, and Pb were 1.44, 1.82, and 1.28 times as high as the background levels, respectively. According to the EF values, Co, Cr, Cu, Ni, and Zn were mainly natural in origin; in contrast, As, Cd, and Pb were influenced by anthropogenic inputs. Pollution levels of these three elements were middle to high. Based on RI values, 11.2% of the study area was under considerable potential ecological risk due to potentially toxic element pollution, whereas the remaining area had low or moderate ecological risk. Spatial correlations between the studied elements depended on spatial scales, which indicates that traditional correlation coefficients did not reflect the real interrelationships among the elements. Parent materials were the main factor that influenced the structure variations of nine elements at both the short- and long-range scales. At the short-range scale, phosphorus-related industrial activities increased the values of Cd, Zn, As, and Pb, and the polluted Hanjiang River resulted the higher values of Cd and Zn in regions near the river. These results should be taken into account when establishing policies for protecting the soil quality of the study area.

Acknowledgments

This study was supported by The Major Science and Technology Program for Water Pollution Control and Treatment (2013ZX0750300104), The National High Technology Research and Development Program of China (2013AA01A608), and China Torch Program (2012GH722002), National Natural Science Foundation of China (41402052, 41601549) and Natural Science Foundation of Hubei Province, China (2013CFB062).

References

Benamghar, A., Gómez-Hernández, J.J., 2014. Factorial kriging of a geochemical dataset for heavy-metal spatial-variability characterization. Environ. Earth Sci. 71, 3161–3170.

Cai, L.M., Xu, Z.C., Bao, P., He, M., Dou, L., Chen, L.G., Zhou, Y.Z., Zhu, Y.G., 2015. Multivariate and geostatistical analyses of the spatial distribution and source of arsenic and heavy metals in the agricultural soils in Shunde, Southeast China. J. Geochem. Explor. 148, 189–195.

Cambardella, C.A., Moorman, T.B., Novak, J.M., Parkin, T.B., Karlen, D.L., Turco, R.F., Konopka, A.E., 1994. Field-scale variability of soil properties in central Iowa soils. Soil Sci. Soc. Am. J. 58, 1501–1511.

Chen, T., Liu, X.M., Zhu, M.Z., Zhao, K.L., Wu, J.J., Xu, J.M., Huang, P.M., 2008. Identification of trace element sources and associated risk assessment in vegetable soils of the urban-rural transitional area of Hangzhou, China. Environ. Pollut. 151, 67–78.

Chen, J.Q., Wang, Z.X., Wu, X., Zhu, J.J., Zhou, W.B., 2011. Source and hazard identification of heavy metals in soils of Changsha based on TIN model and direct exposure method. Trans. Nonferrous Metals Soc. China 21, 642–651.

Chen, H.Y., Zhou, Y.L., Ai, Y.C., Ren, K.J., Yuan, Y.H., Gao, S.Z., 2012. Mine geological environmental problems and control measures of resource-exhausted cities. Resour. Environ. Eng. 26, 259–262 (in Chinese).

Chilès, J.P., Delfiner, P., 1999. Geostatistics: Modeling Spatial Uncertainty. John Wiley & Sons, New York.

Davies, B.E., 1997. Heavy metal contaminated soils in an old industrial area of Wales, Great Britain: source identification through statistical data interpretation. Water Air Soil Pollut. 94, 85–98.

Facchinelli, A., Sacchi, E., Mallen, L., 2001. Multivariate statistical and GIS-based approach to identify heavy metal sources in soils. Environ. Pollut. 114, 313–324.

Gao, B.F., He, L., Zhang, Z., Gan, J.H., 2011. Indicative function of Bellamya aeruginosa in the middle and lower stream of Hanjiang River. Hubei Agric. Sci. 50, 128–131 (in Chinese).

Goovaerts, P., 1992. Factorial kriging analysis: a useful tool for exploring the structure of multivariate spatial soil information. J. Soil Sci. 43, 597–619.

Hakanson, L., 1980. An ecological risk index for aquatic pollution control.a sedimentological approach. Water Res. 14, 975–1001.

Islam, S., Ahmed, K., Al-Mamun, H., 2015. Distribution of trace elements in different soils and risk assessment: a case study for the urbanized area in Bangladesh. J. Geochem. Explor. 158, 212–222.

Lei, P., Zeng, Z.X., Zhang, H., Gao, Z.J., 2015. Risk characteristics of nutrients and heavy metals in the sediments from the branches of Xiangyang section, Hanjiang River. Acta Sci. Circumst. 35, 1374–1382 (in Chinese).

Li, X.Y., Liu, L.J., Wang, Y.G., Luo, G.P., Chen, X., Yang, X.L., Hall, M.H.P., Guo, R.C., Wang, H.J., Cui, J.H., He, X.Y., 2013. Heavy metal contamination of urban soil in an old industrial city (Shenyang) in Northeast China. Geoderma 192, 50–58.

Lin, Y.P., Cheng, B.Y., Shyu, G.S., Chang, T.K., 2010. Combining a finite mixture distribution model with indicator kriging to delineate and map the spatial patterns of soil heavy metal pollution in Chunghua County, central Taiwan. Environ. Pollut. 158, 235–244.

Lin, W.C., Lin, Y.P., Wang, Y.C., 2016. A decision-making approach for delineating sites which are potentially contaminated by heavy metals via joint simulation. Environ. Pollut. 211, 98–110.

Liu, F.Z., Ma, J.Q., 2012. Handbook of Soil Monitoring and Analysis. Chemical Industry Press, Beijing.

Liu, E.F., Shen, J., 2014. A comparative study of metal pollution and potential eco-risk in the sediment of Chaohu Lake (China) based on total concentration and chemical speciation. Environ. Sci. Pollut. Res. Int. 21, 7285–7295.

Liu, Y., Lv, J.S., Zhang, B., Bi, J., 2013. Spatial multi-scale variability of soil nutrients in relation to environmental factors in a typical agricultural region, Eastern China. Sci. Total Environ. 450–451, 108–119.

Luo, W., Lu, Y.L., Giesy, J.P., Wang, T.Y., Shi, Y.J., Wang, G., Xing, Y., 2007. Effects of land use on concentrations of metals in surface soils and ecological risk around Guanting Reservoir, China. Environ. Geochem. Health 29, 459–471.

Lv, J.S., Liu, Y., Zhang, Z.L., Dai, J.R., 2013. Factorial kriging and stepwise regression approach to identify environmental factors influencing spatial multi-scale variability of heavy metals in soils. J. Hazard. Mater. 261, 387–397.

Lv, J.S., Liu, Y., Zhang, Z.L., Dai, B., 2014. Multivariate geostatistical analyses of heavy metals in soils: spatial multi-scale variations in Wulian, Eastern China. Ecotoxicol. Environ. Saf. 107, 140–147.

Lv, J.S., Liu, Y., Zhang, Z.L., Dai, J.R., Dai, B., Zhu, Y.C., 2015. Identifying the origins and spatial distributions of heavy metals in soils of Ju country (Eastern China) using multivariate and geostatistical approach. J. Soils Sediments 15, 163–178.

Mihailović, A., Budinski-Petković, L., Popov, S., Ninkov, J., Vasin, J., Ralević, N.M., Vučinić Vasić, M., 2015. Spatial distribution of metals in urban soil of Novi Sad, Serbia: GIS based approach. J. Geochem. Explor. 150, 104–114.

Mirzaei, R., Ghorbani, H., Hafezi Moghaddas, N., Martín, J.A.R., 2014. Ecological risk of heavy metal hotspots in topsoils in the Province of Golestan, Iran. J. Geochem. Explor. 147, 268–276.

Nanos, N., Rodríguez Martín, J.A., 2012. Multiscale analysis of heavy metal contents in soils: spatial variability in the Duero river basin (Spain). Geoderma 189–190, 554–562.

Nanos, N., Grigoratos, T., Rodríguez Martín, J.A., Samara, C., 2015. Scale-dependent correlations between soil heavy metals and As around four coal-fired power plants of northern Greece. Stoch. Env. Res. Risk A. 29, 1531–1543.

Pebesma, E.J., 2004. Multivariable geostatistics in S: the gstat package. Comput. Geosci. 30, 683–691.

Rodríguez, J.A., Nanos, N., Grau, J.M., Gil, L., López-Arias, M., 2008. Multiscale analysis of heavy metal contents in Spanish agricultural topsoils. Chemosphere 70, 1085–1096.

Schneider, A.R., Morvan, X., Saby, N.P.A., Cancès, B., Ponthieu, M., Gommeaux, M., Marin, B., 2016. Multivariate spatial analyses of the distribution and origin of trace and major elements in soils surrounding a secondary lead smelter. Environ. Sci. Pollut. Res. Int. 23, 15164–15174.

SEPAC, 1995. Environmental Quality Standard for Soil (GB 15618-1995). Standards Press of China, Beijing.

Sollitto, D., Romic, M., Castrignanò, A., Romic, D., Bakic, H., 2010. Assessing heavy metal contamination in soils of the Zagreb region (Northwest Croatia) using multivariate geostatistics. Catena 80, 182–194.

Wang, H.Y., Lu, S.G., 2011. Spatial distribution, source identification and affecting factors of heavy metals contamination in urban-suburban soils of Lishui city, China. Environ. Earth Sci. 64, 1921–1929.

Wang, L.F., Yang, L.Y., Kong, L.H., Li, S., Zhu, J.R., Wang, Y.Q., 2014. Spatial distribution, source identification and pollution assessment of metal content in the surface sediments of Nansi Lake, China. J. Geochem. Explor. 140, 87–95.

Wu, C.F., Zhang, L.M., 2010. Heavy metal concentrations and their possible sources in paddy soils of a modern agricultural zone, southeastern China. Environ. Earth Sci. 60, 45–56.

Wu, S., Peng, S.Q., Zhang, X.X., Wu, D.L., Luo, W., Zhang, T.B., Zhou, S.G., Yang, G.Y., Wan, H.F., Wu, L.Q., 2015. Levels and health risk assessments of heavy metals in urban soils in Dongguan, China. J. Geochem. Explor. 148, 71–78.

Xu, X.H., Zhao, Y.C., Zhao, X.Y., Wang, Y.D., Deng, W.J., 2014. Sources of heavy metal pollution in agricultural soils of a rapidly industrializing area in the Yangtze Delta of China. Ecotoxicol. Environ. Saf. 108, 161–167.

Yuan, H.M., Song, J.M., Li, X.G., Li, N., Duan, L.Q., 2012. Distribution and contamination of heavy metals in surface sediments of the South Yellow Sea. Mar. Pollut. Bull. 64, 2151–2159.

Yuan, G.L., Sun, T.H., Han, P., Li, J., Lang, X.X., 2014. Source identification and ecological risk assessment of heavy metals in topsoil using environmental geochemical mapping: Typical urban renewal area in Beijing, China. J. Geochem. Explor. 136, 40–47.

Zhang, X.Y., Lin, F.F., Wong, M.T.F., Feng, X.L., Wang, K., 2009. Identification of soil heavy metal sources from anthropogenic activities and pollution assessment of Fuyang County, China. Environ. Monit. Assess. 154, 439–449.

Zhao, J., Chu, F., Jin, X., Wu, Q., Yang, K., Ge, Q., Jin, L., 2015. The spatial multiscale variability of heavy metals based on factorial kriging analysis: a case study in the northeastern Beibu Gulf. Acta Oceanol. Sin. 34, 137–146.